UC Davis
San Francisco Estuary and Watershed Science

Title
Variation of Fish Habitat and Extent of the Low-Salinity Zone with Freshwater Flow in the San Francisco Estuary

Permalink
https://escholarship.org/uc/item/3pz7x1x8

Journal
San Francisco Estuary and Watershed Science, 11(4)

Authors
Kimmerer, Wim J.
MacWilliams, Michael L.
Gross, Edward S.

Publication Date
2013

DOI
https://doi.org/10.15447/sfews.2013v11iss4art1

Peer reviewed

Variation of Fish Habitat and Extent of the Low-Salinity Zone with Freshwater Flow in the San Francisco Estuary

Wim J. Kimmerer*, Michael L. MacWilliams[1], and Edward S. Gross[2]

ABSTRACT

We used the UnTRIM San Francisco Bay–Delta hydrodynamic model to examine the spatial distribution of salinity as a function of freshwater flow in the San Francisco Estuary. Our particular focus was the covariation of flow with the spatial extent of the low-salinity zone (LSZ: salinity = 0.5 to 6), and with the extent of habitat for common species of nekton as defined by their salinity ranges. The UnTRIM model has an unstructured grid which allowed us to refine earlier estimates of the availability of suitable salinity ranges, particularly for species resident in low salinity. The response of the salinity field to flow was influenced by the bathymetry of the estuary. Area and volume of the LSZ were bimodal with X2, the distance up the axis of the estuary to a near-bottom salinity of 2, roughly the middle of the LSZ. The smallest area and volume occurred when the LSZ was in the Delta or Carquinez Strait, moderate values when it was in Suisun Bay, and the highest values when it was in broad, shallow San Pablo Bay. Resource selection functions for the distributions of common nekton species in salinity space were updated from previous values and used to calculate

salinity-based habitat indices using the UnTRIM results. These indices generally increased with decreasing X2 (increasing flow), but the slopes of these relationships were mostly inconsistent with corresponding relationships of abundance to flow. Thus, although the salinity range used by most nekton expands as flow increases, other mechanisms relating population size to flow are likely more important than the physical extent of suitable salinity.

KEY WORDS

Salinity, habitat, fish, freshwater flow, resource selection function, delta smelt, longfin smelt, striped bass, threadfin shad

INTRODUCTION

Salinity is crucial in determining the distributions of nearly all species that inhabit estuaries. Although salinity (or conductivity) is but one of many attributes that define habitat, most estuarine species are abundant within a limited range of salinity. As this salinity range moves with freshwater and tidal flows, attributes of this habitat may change, including its spatial extent, local bathymetry, exchange processes, and biotic interactions. These changes may, in turn, alter population dynamics of the species so as to cause abundance to covary with freshwater flow on

* Corresponding author: Romberg Tiburon Center, San Francisco State University, 3152 Paradise Drive Tiburon, CA 94920 USA; *kimmerer@sfsu.edu*
1 Delta Modeling Associates, Inc., San Francisco, CA USA
2 Resources Management Associates, Inc., Berkeley, CA USA

an annual time scale (Kimmerer 2002b). Here we ask how the extent of habitat defined by salinity varies with freshwater flow, and whether this covariation may cause variation in abundance with flow.

A river-dominated estuary can be considered an ecocline with two ecotones, i.e., ecosystem properties such as species composition vary slowly with salinity within the gradient but the ends of the gradient can be a sharp barrier for both freshwater and marine species (Attrill and Rundle 2002; Greenwood 2007). Efforts to classify estuarine salinity ranges into discrete units on the basis of distributions of biota, beginning with the Venice classification system, have met with mixed success (Bulger et al. 1993, Greenwood 2007). Nevertheless, many such systems identify a low-salinity or oligohaline zone as an important region for a variety of physical, chemical, and biological properties (Postma and Kalle 1955; Morris et al. 1978; Baross et al. 1994; North and Houde 2003). Influences of freshwater flow on the biota of estuaries often occur indirectly through the response of salinity and its covariates. For example, salinity stratification can stimulate primary production (Cloern 1984). Shifts in the salinity field can alter the distribution and abundance of benthic filter feeders, resulting in variation of phytoplankton with flow (Nichols 1985; Wilber 1992). In addition the distributions of marsh and submerged plants can shift during long periods of altered salinity (Watson and Byrne 2009).

The salinity field of a tidal estuary with strong river flow is influenced by freshwater flow into the estuary, and by mixing processes that lead to salt intrusion from the ocean. These mixing processes include tidal dispersion (Zimmerman 1986) and gravitational circulation (Monismith et al. 2002). The relative strength of each of these processes varies spatially because of the spatially variable bathymetry of the estuary, and it varies in time and space depending on the location and movement of salinity gradients (Gross et al. 2010). In the vertical direction, turbulent mixing is the dominant mixing process and it interacts strongly with gravitational circulation (Monismith et al. 2002). The result of the interplay between net seaward advection by tributary inflows and horizontal and vertical mixing processes is a

complex and time-varying circulation and salinity field that can include both stratified and vertically well-mixed conditions at different times and locations.

The spatial distribution of salinity in a river-dominated tidal estuary is, therefore, difficult to determine using monitoring data alone. This is clearly the case in the San Francisco Estuary (estuary), with its long records of salinity measurement. Continuous monitoring gives good temporal resolution but poor spatial resolution, and measurements can vary with small differences in positions of the sensors. Vessel-based sampling confounds space and time and usually results in a relatively small number of measurements. Although continuous spatial records have been taken (e.g., Powell et al. 1989), they have proved difficult to interpret and have not contributed much to knowledge about the estuary.

Three-dimensional (3-D) hydrodynamic models provide an alternative means to determine patterns of salinity in an estuary. Field measurements are used for calibration but otherwise the model can be run independently of measurements if suitable boundary conditions are available. If the model is calibrated over the range of salinity conditions in the region of interest, the salinity predictions should be as accurate as the calibration.

Previously we used the 3-D version of the TRIM model (Casulli and Cattani 1994; Gross et al. 2010) to examine salinity distributions in the estuary and in particular how the availability of habitat for various species of nekton, based on salinity and depth, varied with freshwater flow (Kimmerer et al. 2009). The principal conclusion was that increases in the extent of this habitat with flow were probably unrelated to increases in population size of most of the species examined. At that time, the TRIM model was the best-calibrated 3-D model of the estuary, but it lacked resolution in narrow channels and represented most of the Sacramento–San Joaquin Delta as a pair of shallow tidal lagoons. This was a drawback for analyzing the habitat of fish species that spend much of their time in freshwater.

In this paper we re-examine the distribution of salinity in the estuary using UnTRIM (Casulli and

Zanolli 2002, 2005), a successor to TRIM that uses an unstructured grid and is therefore capable of representing the network of narrow channels in the Delta. This model has been implemented and calibrated for the Estuary and used in several management-related applications (MacWilliams et al. 2008, unpublished). We ran the model with nine different steady values of Delta outflow, supplemented with output from a 3-year period from April 1994 through March 1997 that included the calibration period (MacWilliams et al. unpublished). Our particular focus was on the low-salinity zone (LSZ), defined here by a salinity range of 0.5 to 6 (Practical Salinity Scale), because of its importance as habitat for delta smelt (Bennett 2005) and because it has been the focus of numerous studies of circulation, organism retention, and plankton dynamics (e.g., Arthur and Ball 1979; Burau 1998; Kimmerer et al. 1998, 2012). We asked how the spatial extent (volume, area, depth) of this zone varied with flow, and whether a better-defined and more extensive analysis of the extent of the salinity ranges of various nekton species would cause us to alter our earlier conclusions (Kimmerer et al. 2009).

We use X2, the distance in km up the axis of the estuary to a near-bottom tidally averaged salinity of 2, as a measure of the physical response of the estuary to freshwater flow. X2 is related to abundance indices of several estuarine nekton species (Jassby et al. 1995; Kimmerer 2002a). The LSZ is centered at a salinity of about 2; thus, X2 is a measure of the position of the LSZ. However, it is important to distinguish between the LSZ as a particular habitat and the numerical value of X2 as a measure of the wide variety of the physical responses of the estuary to flow (Kimmerer 2002b). In particular, abundance of various fish species may respond to X2 or its correlates through mechanisms that are not directly related to LSZ characteristics (Kimmerer 2002b; Kimmerer et al. 2009).

This paper examines the distribution of salinity from several perspectives. We examined the influence of both steady and time-varying flows on the area and volume of the LSZ. Steady flows used to set up this analysis were based on values for summer–fall (July through October) because of current interest in this period in the life cycle of delta smelt (Bennett 2005), but the results apply to the range of flows regardless of season. We also refined the previous analyses of the relationship of resource selection functions to flow and X2 (Manly et al. 2002; Kimmerer et al. 2009) using the finer resolution provided by UnTRIM to investigate the low-salinity end of the system. We analyzed data for species included in the previous study (Table 1), selected because they are abundant or because they have relationships of abundance to X2 as described in Jassby et al. (1995) and Kimmerer et

Table 1 Species analyzed with sampling programs that provided data for each of the habitat indices, and months included in each analysis. Sampling programs are: the 20mm survey (20mm, Dege and Brown 2004), Summer Townet Survey (TNS, Turner and Chadwick 1972), Fall Midwater Trawl Survey (FMWT, Moyle et al. 1992), and the San Francisco Bay Study midwater trawl (Bay MW) and otter trawl (Bay OT, Armor and Herrgesell 1985).

Common name	Scientific name	Sampling program	Months
Bay shrimp	*Crangon franciscorum*	Bay OT	May–Nov
Starry flounder	*Platichthys stellatus*	Bay OT	May–Nov
Northern anchovy	*Engraulis mordax*	MWT, Bay MW	Sep–Dec, Apr–Nov
Longfin smelt	*Spirinchus thaleichthys*	MWT, Bay MW	Sep–Dec, May–Dec
Delta smelt	*Hypomesus transpacificus*	20mm, TNS, MWT	Mar–Jul, Sep–Dec
American shad	*Alosa sapidissima*	MWT, Bay MW	Sep–Dec , May–Nov
Threadfin shad	*Dorosoma petenense*	20mm, TNS, MWT	Mar–Jul, Jun–Aug, Sep–Dec
Striped bass	*Morone saxatilis*	20mm, TNS, MWT, Bay MW, Bay OT	Mar–Jul, Jun–Aug, Sep–Dec, May–Dec

al. (2009). In this study we included threadfin shad, which could not be analyzed before because its habitat is mainly in freshwater, and omitted Pacific herring, which lacks a significant relationship with X2.

METHODS

Model Summary

UnTRIM (Casulli and Zanolli 2002, 2005) is an extension of the 3-D hydrodynamic model TRIM, which has been widely used in the estuary and elsewhere (Gross et al. 1999, 2010; Kimmerer et al. 2009). UnTRIM uses an unstructured grid, which has several advantages over the Cartesian grid used in TRIM. The grid can be made finer to resolve narrow channels and other small features of interest and coarser elsewhere, focusing computer resources where they are needed. Grid cells can be oriented along the axes of sinuous channels, making the model's representation of spatially continuous flow more accurate. In addition, grid cells can be made narrow enough to represent even small channels with at least a few rows of cells, improving accuracy in narrow channels.

The UnTRIM Bay–Delta model represents the entire San Francisco Estuary from the landward reaches of the Sacramento–San Joaquin Delta to the Gulf of the Farallones (MacWilliams et al. unpublished). In our application of the model, the grid is coarse in the ocean and gradually becomes finer, with the finest resolution in the Delta. The model has been calibrated using water level, velocity, flow, and salinity data collected throughout the estuary (MacWilliams et al. 2008, unpublished). The calibration period of April 1994 through March 1997 was selected because substantial field data on salinity and velocity were available from the Entrapment Zone study (Burau 1998; Kimmerer et al. 1998, 2002; Bennett et al. 2002). This period also encompassed a wide range of freshwater flows, from daily Delta outflow of 20 m^3 s^{-1} in October 1994 to 11,500 m^3 s^{-1} in March 1995.

Following the approach used by Kimmerer et al. (2009), nine steady outflow scenarios were simulated that spanned a range of outflows. Six flows were selected to achieve an approximately even

distribution of calculated X2 values, resulting in a roughly log–equal interval of flow spanning 100 to 2,810 m^3 s^{-1}. Three additional intermediate flow values (140, 265, and 520 m^3 s^{-1}) were added to better represent changes in salinity-based habitat as a function of X2 through Suisun Bay (Table 2). The lowest flow is in the 12th percentile of daily flows from the DAYFLOW[1] data set from water years 1956 through 2011 and the 17th percentile of dry-season (May through November) flows. The high flow is in the

Table 2 Outflow and steady-state X2 for each constant flow scenario and the time (d) for X2 to move halfway from an initial position to its steady-state value.

Outflow (m^3 s^{-1})	X2 (km)	T1/2
100	89.8	25.4
140	84.8	23.1
190	79.4	22.8
265	72.8	18.3
370	67.4	14.6
520	62.5	9.4
730	57.9	7.0
1440	50.6	4.3
2810	42.7	2.1

94th percentile of flows for the whole year and the 99.5th percentile of dry-season flows. The times to reach steady state in these model runs were inversely related to outflow (Table 2).

Boundary Conditions

MacWilliams et al. (unpublished) describe all of the boundary conditions used in the UnTRIM Bay–Delta model. The discussion here summarizes the boundary conditions specific to the steady outflow scenarios. These were designed to use repeating conditions over each day, eliminating the need to average over the spring–neap tidal cycle to represent steady-state conditions. We used a constant salinity of 33.5 at

---

1 DAYFLOW is a DWR developed program to estimate average daily flows for the Delta and its tributaries through measurements and calculations *http://www.water.ca.gov/dayflow/* [accessed 30 April 2011].

Table 3 Inflows ($m^3 s^{-1}$) from each river for each steady outflow scenario. All values based on DAYFLOW.

River flows	Outflows ($m^3 s^{-1}$)								
	100	140	190	265	370	520	730	1440	2810
Cosumnes	0.8	0.8	0.9	1.1	1.3	1.5	1.9	3.2	5.8
Calaveras	4.0	4.4	4.9	5.7	6.7	8.2	10	17	31
Mokelumne	6.8	7.5	8.4	9.6	11	14.0	18	30	54
Sacramento	332	364	405	467	553	676	848	1431	2555
San Joaquin	56	62	69	79	94	115	144	244	435
Yolo	4.6	5.0	5.6	6.5	7.6	9.3	12	20	35
Total inflow	404	444	494	569	674	824	1034	1744	3114

the ocean boundary and a repeating daily tide comprising the M2 lunar semidiurnal tidal component modified to a 12-hr period and the K1 lunar diurnal component modified to 24 hr. These were phased such that lower low water followed higher high water as in the estuary. Wind and evaporation also varied repetitively over each 24-hr period to represent the average summer daily pattern of meteorological conditions. Historical data from July through October during water years 1980 through 2010 were used except as noted below. Output from the DAYFLOW program for July through October during water years 1980 through 2010 was used to calculate the proportion of total inflow from each river (Table 3), the long-term mean export rate (237 $m^3 s^{-1}$), and the proportion of total water exports attributable to each export facility (Table 4). Export rates for the Contra Costa Water District diversion were apportioned between the Rock Slough (39%) and Old River (61%) intakes. Delta Island Consumptive Use (DICU) was determined for the same period for each of 257 DICU nodes, with a total net withdrawal of 67 $m^3 s^{-1}$. For all scenarios, Delta exports and DICU remained constant, and inflow was calculated to achieve the target outflow. Mean discharges of streams flowing directly into the estuary west of the Delta were estimated from available gage data from July through October of 1990 through 2010, adjusted by the ratio of total-to-gaged watershed area of each stream. The total of these inflows was 6.9 $m^3 s^{-1}$, about 94% of which flows into South Bay and most of the remainder into San Pablo Bay.

Table 4 Average Delta export flows for July through October of water years 1980 to 2010 used in the steady-flow scenarios. Export flows are for water pumped out of the Delta for agricultural and municipal uses.

Export facility	Average flow ($m^3 s^{-1}$)	Percent (%) contribution
State Water Project	121	51
Central Valley Project	110	46
Contra Costa Water District	5.5	2.3
North Bay Aqueduct	1.7	0.7
Total export flow	237	

For the steady outflow scenarios, we assumed typical summer operating conditions for all control structures in the Delta. The Delta cross-channel and Suisun Marsh salinity control gate were open; the barrier at the head of Old River was open; and the three temporary barriers on Grant Line Canal, Middle River, and Old River at the Delta–Mendota Canal were in place with culverts and weirs operating under typical summer configurations.

Model Runs and Analysis

For each steady flow, the model was run for 180 days to reach steady state. X2 for each steady flow was determined from the distribution of bottom salinity during the steady-state run. Model results were averaged over the last day of each simulation. The distributions of salinity and depth in each of six model regions (one region—the ocean—was not used in most of the calculations) were summarized from

the model as matrices of surface area in the region for each combination of 80 bins of salinity and 56 bins of depth. Salinity bins were in increments of 1 above 5, and 0.1 below 5. Depth bin increments were 1 m from 0 to 40 m (encompassing 97% of the volume of the estuary), and 5 m from 40 m to 100 m.

Areas of each bin in the matrix were multiplied by the midpoint depths of the bins to determine volumes which were summed over all depths in the salinity range. To analyze the characteristics of the LSZ, we summed volumes and areas of all cells in San Pablo Bay, Suisun Bay, and the Delta with salinity between 0.5 and 6, and calculated the mean depth as the ratio of volume to area. A similar calculation using model output from April 1994 through March 1997, which included the calibration period, was used to compare the steady-state and time-varying cases. We also developed a hypsograph of area vs. depth for each region at an intermediate flow (370 m^3 s^{-1}).

Resource selection functions to estimate area and volume of the salinity ranges used by species of nekton were updated from Kimmerer et al. (2009) using monitoring data through 2010. Briefly, generalized additive models (GAMs) were fit to data on catch per trawl or frequency of occurrence as a function of salinity. GAMs were fit using a loess smoother with degree = 2 and span = 0.5, and either a Poisson (catch per trawl) or binomial (frequency of occurrence) error distribution. In the previous analysis we used depth as a covariate with data from the Bay Study otter trawl (Kimmerer et al. 2009). We did not do so here because that analysis showed effects only in deep, saline waters (Kimmerer et al. 2009) and here we focused more on the freshwater end of the system. We calculated resource selection functions using data from all stations except that data from the 20-mm Survey and Summer Townet Survey (TNS) were restricted to Suisun Bay and the Delta because of limited coverage in San Pablo Bay. Twenty-five bootstrap samples were taken for each resource selection function to allow for approximate error estimates.

Resource selection functions were standardized to the range (0,1) and used as weighting factors with the data on total volume by salinity to calculate salinity-based habitat indices (hereafter, habitat indices) for

the entire estuary for each species at each of the nine steady-flow levels. Combinations of species and sampling programs were included only if the sampling programs covered most of the salinity range of the species; for example, northern anchovy collected by the TNS was excluded since most of the fish occur seaward of the region sampled by this program.

The statistic of interest from this analysis was the slope of the relationship between the log of the habitat index and X2. To the extent that this slope matched that of the corresponding relationship of log of abundance index to X2 (Jassby et al. 1995; Table 2 in Kimmerer et al. 2009), the result would support the flow-based change in extent of suitable salinity (the habitat index) as a mechanism for the response of abundance index to flow (under the assumption that population size would scale with area of suitable salinity). A more negative slope for the log abundance–X2 relationship would imply that other mechanisms besides variation in extent of suitable salinity were contributing to the flow response of abundance. A more negative slope for the log habitat–X2 relationship would imply that fish abundance was unresponsive to volume or area of the habitat as defined by the salinity field.

RESULTS

The hypsographs show the predominance of shallow water in all regions of the estuary (Figure 1). The median depth is 6.3 m in Central Bay and < 4 m in the other regions. Even the Delta is predominantly shallow, although the western Delta near the confluence of the Sacramento and San Joaquin rivers is deeper than farther eastward (not shown).

Spatial distributions of salinity with flow (Figure 2) show both the movement of the salinity field and the change in its shape and characteristics. At a low flow of 140 m^3 s^{-1} (X2 = 85 km) the low-salinity zone is in the western Delta, Suisun Bay has salinity up to ~15, and San Pablo to Central Bay are at salinity close to seawater. At a flow of 1,440 m^3 s^{-1} (X2 = 51 km) Suisun Bay is fresh and the LSZ is in the shoals of San Pablo Bay. Although stratification cannot be seen in these maps of depth-averaged salinity, it can be inferred from the higher salinity in channels than
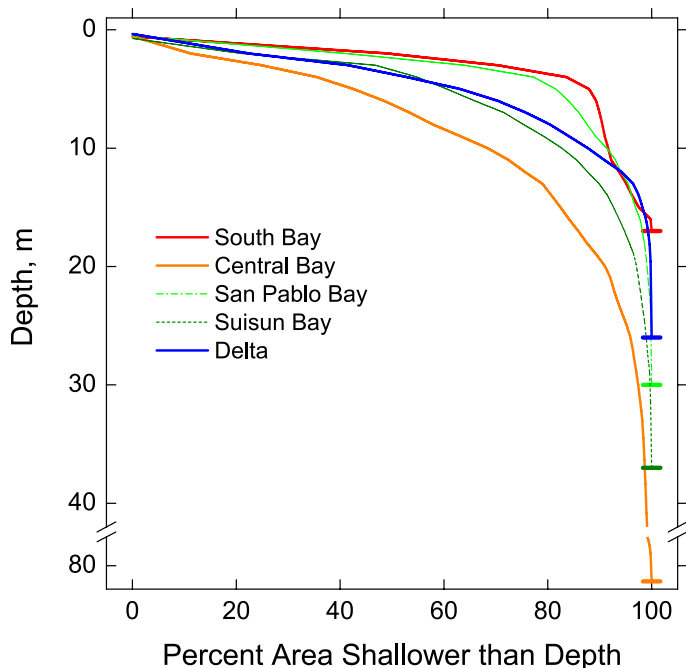
Figure 1 Hypsograph by basin for the San Francisco Estuary, giving cumulative percentage of area deeper than each 0.1-m increment of depth below the NAVD88 datum
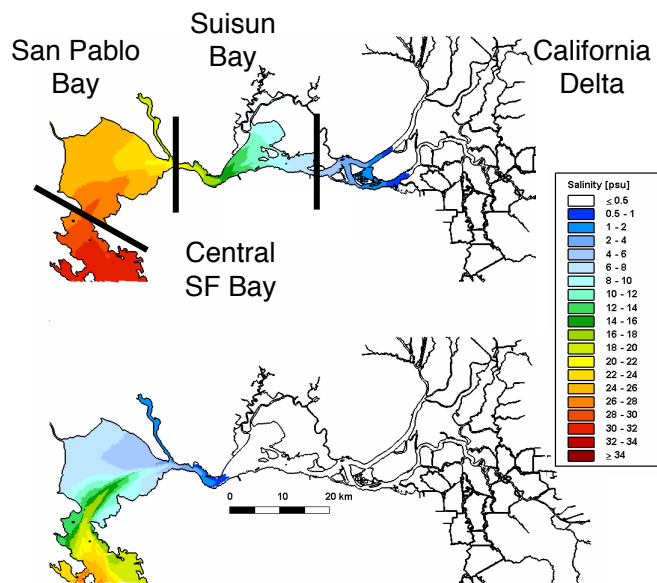
Figure 2 Maps of the northern San Francisco Estuary showing regions and boundaries (black lines). Modeled depth- and daily-averaged salinity for two steady flow scenarios. **Top**: 140 m^3 s^{-1}. **Bottom**: 1,440 m^3 s^{-1}, close to the 20th and 80th percentiles, respectively, of monthly mean Delta outflow from water years 1956 through 2011.
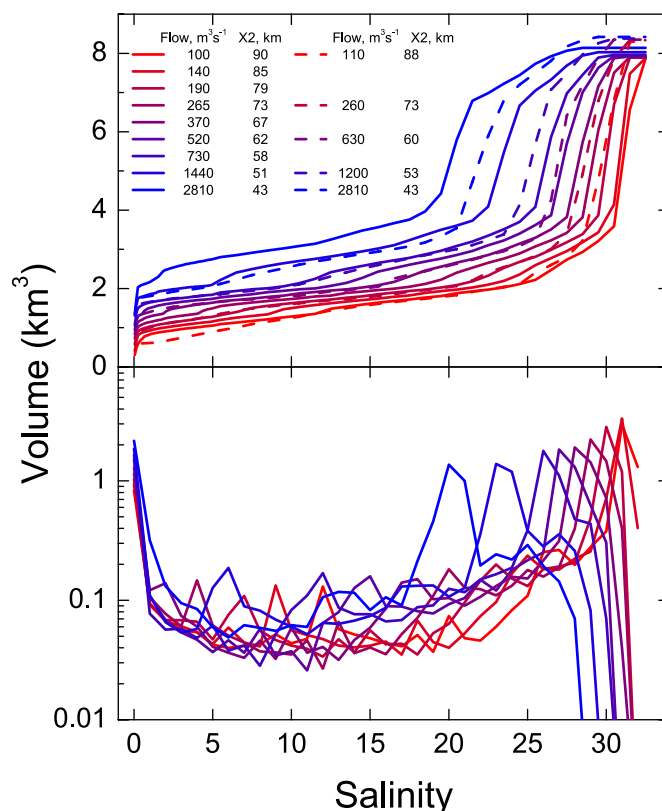
Figure 3 Top: cumulative volume by salinity bin from the UnTRIM model at 9 steady flows (solid lines) and the TRIM model at 5 steady flows (dashed lines). **Bottom:** volume by salinity in increments of 1 unit from UnTRIM. Flows and corresponding X2 values are color-coded with red representing the driest and blue the wettest conditions. Volumes are relative to mean sea level, binned according to water-column mean salinity. Lines for TRIM results have an additional volume of 0.6 km^3 added to account for the unresolved portion of the Delta, assumed to be freshwater.

adjacent shoals in southern San Pablo Bay during the high-flow period.

The distribution of volume by salinity throughout the estuary (Figure 3) reveals several key features using both the UnTRIM results and our previous results with TRIM. First, the largest part of the total volume of the estuary is in deep channels of Central Bay, indicated by the peaks in volume in the lower panel of Figure 3. Second, the total volume of the estuary is bimodal with respect to salinity: about half is within 10 of the maximum salinity, 10% to 20% is

fresh, and the remainder is spread over the remaining salinity range. As flow increases the volume of the freshwater pool increases, the maximum salinity in the estuary decreases, and the salinity in the deep channels of Central Bay decreases still further. Third, as flow increases there is no consistent response of volume in salinity between 1 and 10, and a modest increase in volume between 10 and 25. The volume of freshwater grows faster with flow in results using UnTRIM than in those from TRIM because the Delta is fully resolved in UnTRIM.

The distribution of salinity by basin shows the progressive freshening moving down-estuary as X2 decreases (Figure 4). The Delta is essentially freshwater except at very low flows when brackish water intrudes into the western Delta from Suisun Bay. Suisun and San Pablo bays have the widest range of salinity from freshwater during moderate to high-flow periods to polyhaline during low flow periods. Central and South bays have similar salinity patterns consisting primarily of near-oceanic salinity at low to moderate flows with progressive freshening as flow increases.

The relationships of area and volume of the LSZ to flow or X2 are bimodal (Figure 5). As expected, volume and area of the LSZ increase as the LSZ moves from the western Delta (X2 > 75) into the center of Suisun Bay (X2 ~ 65). However, area and volume then decrease as the LSZ moves further westward through Suisun Bay into Carquinez Strait and then increase sharply around X2 < 50 km. Defining the LSZ by bottom salinity instead of depth-averaged salinity makes little difference in these patterns (Figure 5). Mean depth—the ratio of volume to area—shows a roughly inverse pattern to area, which is more variable than volume. The steady-flow and historical model runs corroborate each other at X2 above about 65 km. At higher flows the area and volume of the LSZ vary widely for a given X2 from the historical run, and this variation is greatest and most divergent when X2 is changing rapidly. In addition, there is a sharp discontinuity in area and volume in the historical model output around X2 = 40.

Updated resource selection functions were similar to those developed previously except that the func-
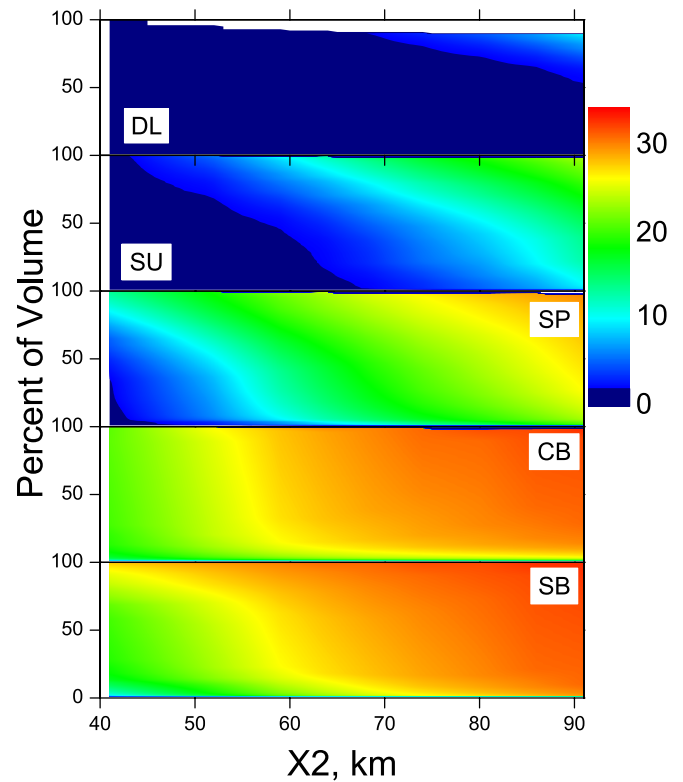

Figure 4 Volume in each region (as percent of the maximum total volume in that region) by X2 with contours indicating depth-averaged salinity. Regions are from northeast to southwest: Delta (DL), Suisun Bay (SU), San Pablo Bay (SP), and Central (CB) and South (SB) San Francisco bays.

tion for threadfin shad was not developed previously (Figure 6). This shows that threadfin shad is the most freshwater-oriented species of the abundant species in the data set. In many cases the resource selection functions based on catch were more tightly confined to a salinity range than those based on frequency of occurrence because of the occasionally high catches in that salinity range.

Examples of the relationships of salinity-based habitat volume to X2 show a reasonably tight fit (Figure 7). Error bars based on bootstrap resampling of the raw data used to develop the GAM curves were small relative to variability across X2 values for most species.

We compared the slopes of log-transformed habitat volume vs. X2 (examples in Figure 7) to corresponding slopes of log abundance vs. X2 simply by

8
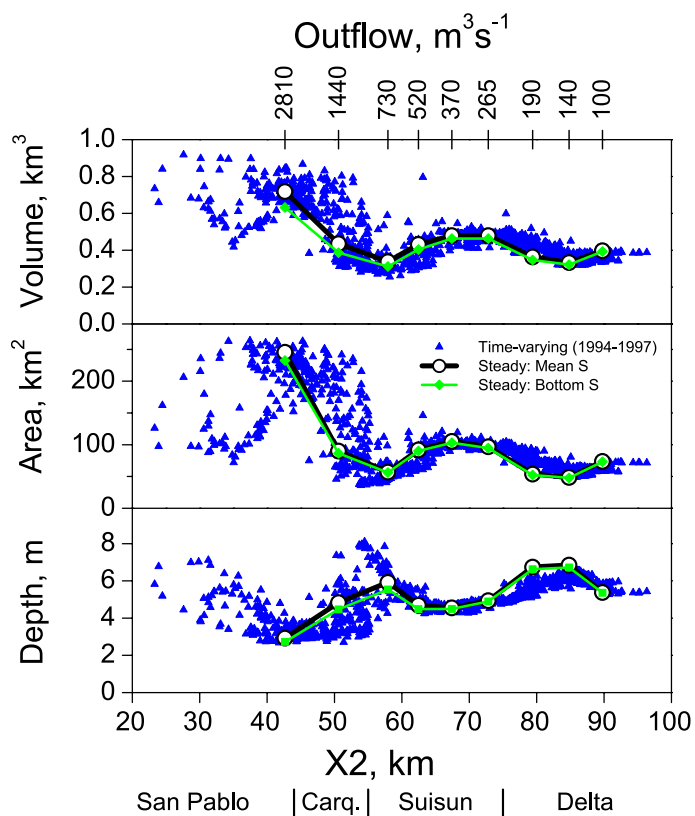
Figure 5 Volume, area, and mean depth (volume * 1000/area) of the Low-Salinity Zone (salinity 0.5 to 6) vs. X2 from the UnTRIM model under nine steady flow scenarios using water-column mean (open circles) or bottom (closed diamonds) salinity. Also shown are daily values based on variable flows during April 1994 through March 1997 (triangles; MacWilliams et al. unpublished). Upper axis gives the Delta outflow corresponding to flow boundary conditions used in the model. Regions of the estuary are indicated at the bottom.
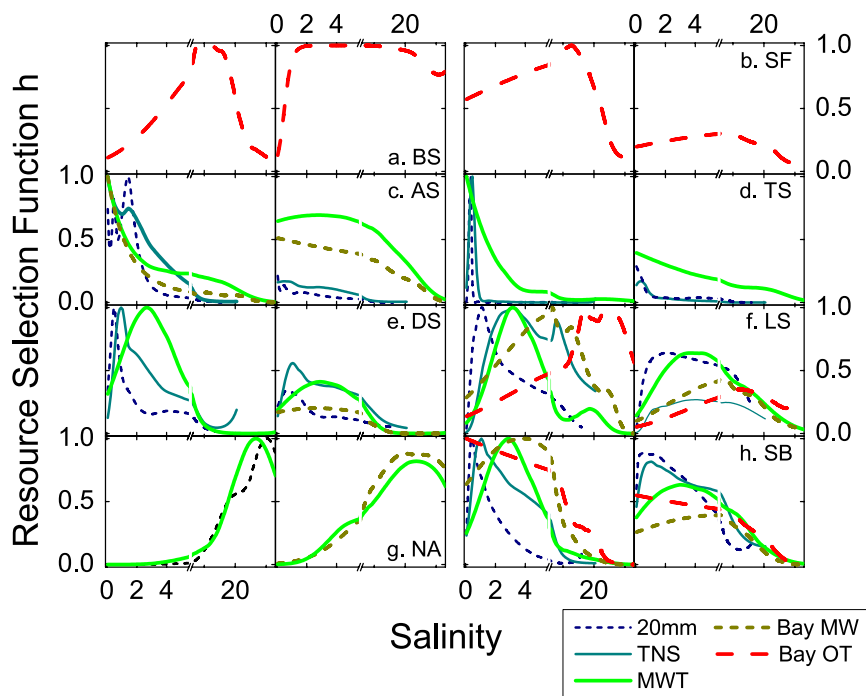
Figure 6 Resource selection functions for abundant species in each of the five sampling programs. The x axis has been broken to emphasize patterns at S < 5.5. Each pair of panels includes lines for a single species based on catch per trawl (left) and frequency of occurrence (right). Species are: a, bay shrimp; b, starry flounder; c, American shad; d, threadfin shad; e, delta smelt; f, longfin smelt; g, northern anchovy; h, striped bass. Sampling programs (legend) are the 20mm Survey, the Summer Townet Survey (TNS), the Fall Midwater Trawl Survey (FMWT), the Bay Study midwater trawl (Bay MW), and the Bay Study otter trawl (Bay OT).
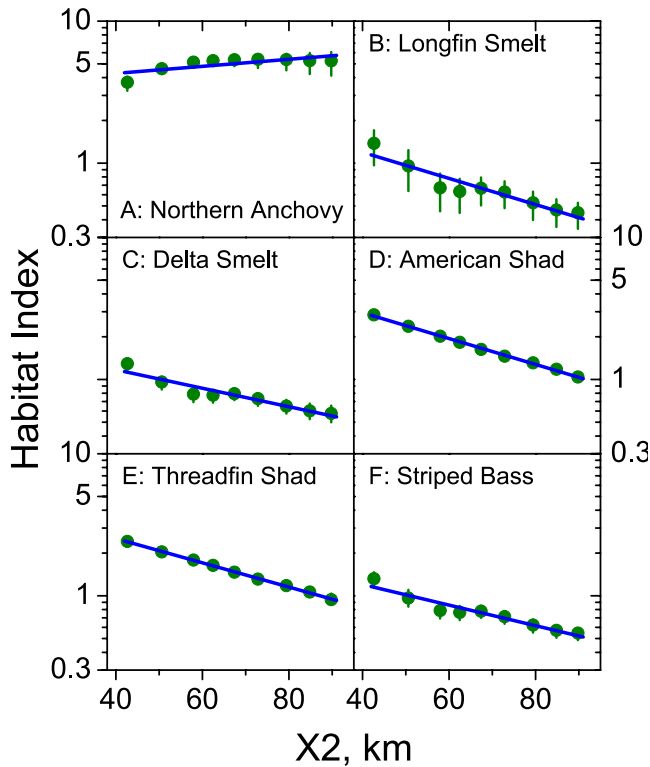
Figure 7 Examples of relationships between X2 and habitat indices. These are for catch per trawl in the Fall Midwater Trawl Survey with salinity averaged through the water column. Each point is the volume by salinity bin, weighted by the resource selection function (Figure 6). Error bars are ranges of each habitat index determined from bootstrap sampling (N = 25) of the raw data in producing the resource selection functions. Lines are least-squares fit to the log-transformed data.

Figure 8 Slopes of relationships between habitat indices based on catch per trawl (blue filled symbols) or frequency of occurrence (green open symbols) vs. X2, from sampling programs indicated by shapes of symbols. The values for catch per trawl from the Fall Midwater Trawl Survey (filled triangles) are the slopes of the lines in Figure 7. Habitat indices were determined by weighting the volume in each salinity interval by the resource selection functions in Figure 6, then calculating total weighted habitat volume for each of the nine steady flows. Confidence limits for slopes of habitat vs. X2 are contained within the symbols except where shown. Red horizontal lines indicate slopes of abundance–X2 relationships with 95% confidence intervals (Kimmerer et al. 2009).

determining whether the habitat slopes fell in or out of the 95% confidence limits of the abundance–X2 slopes (Figure 8). We did not perform statistical tests since the different surveys and different measures (catch vs. frequency of occurrence) have different assumptions and we have no criteria for choosing one over the others. Habitat indices based on the resource selection functions responded to flow as previously observed, i.e., there was a small negative relationship to X2 (positive to flow) for most species in most sampling programs (Figure 7). The principal exception was northern anchovy, because its high-salinity habitat decreases in volume within the estuary as flow increases. Among species known to respond to flow (Kimmerer et al. 2009), habitat–X2 slopes fell within the error bounds of abun-

dance–X2 slopes for starry flounder, striped bass, and American shad (Figure 8). Slopes of habitat index to X2 for longfin smelt were much less negative than abundance–X2 slopes. The slopes of habitat index to X2 for delta smelt and threadfin shad were usually lower than the lower 95% confidence limit of the corresponding abundance–X2 relationships, except for those for catch of threadfin shad in the Summer Townet Survey (TNS) and Fall Midwater Trawl Survey (FMWT). Bay shrimp had flatter relationships of habitat index to X2 than abundance to X2.

DISCUSSION

This study may be the first to examine in such detail the distribution of salinity throughout an estuary as a function of freshwater flow, although similar analyses have been conducted for coastal regions (e.g., Lacroix et al. 2004). It is the first to examine the salinity field at sufficient resolution to quantify the extent of suitable salinities for estuarine organisms throughout their ranges. This kind of analysis in a large estuary of complex bathymetry requires the use of a highly resolved hydrodynamic model, because the necessary spatial resolution could not be obtained with any reasonable number of monitoring stations. The excellent calibration of UnTRIM across a wide range of freshwater flows (MacWilliams et al. unpublished) ensures that model results are suitable for this purpose.

All of the figures taken together illustrate the dynamism and complexity of the spatial-temporal distribution of salinity and conditions in the LSZ. The basin-wide distributions of salinity (Figure 4) indicate that at the scale of whole basins the transitions in salinity are smooth, and that both Suisun and San Pablo bays encompass wide ranges of salinity under most flow conditions. The salinity map for high flow (Figure 2 bottom) shows intrusion of saline water into San Pablo Bay, while low-salinity water spreads throughout the shallows. Deep areas are important as conduits for landward movement of high-salinity water and in promoting stratification (Monismith et al. 2002).

Previous views of the relationship of area and volume of the LSZ to X2 have focused on movement

of the LSZ into the shallows of Suisun Bay, and a consequent increase in its area and decrease in its mean depth (Cloern et al. 1983). Depth has two key biological consequences. A decrease in mean depth can increase phytoplankton growth rate if turbidity does not change, so that shallow areas can be sources of high phytoplankton productivity (Cloern et al. 1983; Lucas et al. 1999). However, grazing by a given biomass of clams removes a greater fraction of phytoplankton biomass in shallow than in deep water, and, since the introduction of *Potamocorbula*, the relationship of phytoplankton production to depth may be positive or negative (Lucas and Thompson 2012). Phytoplankton primary production and specific growth rate in the LSZ did not change appreciably as flow decreased and X2 moved into central Suisun Bay through spring–summer of 2006–2007 (Kimmerer et al. 2012). Thus, the change in shape of the LSZ with its movement does not appear to result in substantial changes in phytoplankton productivity.

Different estuarine species use shallow and deep habitat differently (e.g., Hobbs et al. 2007; Sommer et al. 2008; Grimaldo et al. 2009). Pelagic organisms orient principally to salinity or its covariates (e.g., turbidity, food availability) and geographic features of the habitat may be less important (Dege and Brown 2004). Benthic or littoral species orient to geographic features and their covariates (e.g., depth distribution, aquatic vegetation), although they may shift positions through movement, or by dying back where salinity becomes unfavorable and colonizing elsewhere. Therefore, movement of a water mass with a given salinity range into a shallow area will alter the feeding and predatory environments for pelagic fish through an increase in average light level in that water mass and changes in the relative abundance of food and predators. Thus it is conceivable, though not actually demonstrated, that some fish species may find more favorable conditions for growth when their salinity range is in a predominantly shallow area.

The possibility of higher fish production in shallow than deep water guided our expectation of an increase in area and volume of the LSZ with decreasing X2. However, the observed relationships were more complex and less monotonic than expected

11

(Figure 5). As the LSZ moved from the Delta into Suisun Bay, area and volume increased and mean depth decreased as expected. However, further increases in flow moved the LSZ into Carquinez Strait, squeezing the LSZ into narrow, deep channels and increasing its mean depth. At the highest flow, when the LSZ was in San Pablo Bay, the area and volume of the LSZ were substantially higher than when it was in Suisun Bay.

No species of fish occupies the LSZ completely or exclusively, but several are most abundant in the LSZ (Figure 6). If abundance of these fish tracked their available habitat, the relationship of log abundance index to X2 should resemble the graphs of either area or volume vs. X2 (i.e., Figure 5). However, all of the non-zero relationships of log species abundance index to X2 were linear with no indication of a bimodal pattern (Figure 3 in Kimmerer et al. 2009). This may reflect the infrequent occurrence of very low X2 values over long periods in the historical record: daily X2 was <50 km on only 7% of days in January through June of 1967 through 2010. In addition, the months-long averaging periods used in those analyses would have smoothed the X2–abundance relationships. For example, the averaging period used in the X2–abundance relationship for longfin smelt was January through June, over which there were no values <50 km. Nevertheless, the observed X2–abundance relationships are inconsistent with a mechanism that involves extent of low-salinity habitat, which has a strongly nonlinear relationship to X2 (Figure 5).

The steady-state values of area, volume, and depth of the LSZ generally agreed with those based on the 1994 through 1997 historical model simulation (MacWilliams et al. unpublished). The largest differences occurred during large excursions in flow (Figure 5). These differences mainly resulted from the growing responsiveness of the salinity field to flow at higher values of flow, a feature not previously captured in the flow–X2 relationships (Jassby et al. 1995; Monismith et al. 2002; MacWilliams et al. unpublished). There are also differences at lower flow (higher X2) which probably reflect the autocorrelated response of X2 and, therefore, the entire salinity field to unsteady flow.

The refinements provided by UnTRIM include the ability to represent more accurately the movement of water in channels, both because of the smaller cell sizes relative to models with structured grids, and because the cells can be aligned with the principal local axis of the channels. This means that stratification and salt transport should be captured better in UnTRIM than in models such as TRIM. For example, the distribution of salinity in longitudinal profiles is represented considerably better in UnTRIM (MacWilliams et al. unpublished) than in TRIM (Gross et al. 2010; Figures 6 and 7) for similar hydrologic conditions. Nevertheless, it is encouraging that the differences in results of this analysis and those using TRIM (Kimmerer et al. 2009) were fairly subtle. Threadfin shad lives mainly in freshwater regions of the Delta (Figure 6) and could not be analyzed at all using TRIM because of this lack of resolution in the Delta. The other species whose salinity distributions indicated high abundance in freshwater (Figure 6, e.g., delta smelt, American shad, striped bass) had similar slopes of habitat index to X2 to those in the previous analysis except that the values in this analysis varied less across life stages. This likely also resulted from the better resolution in freshwater, since all of these species shift ontogenetically toward brackish water (Figure 6). The slopes for northern anchovy in this analysis were positive, while in the TRIM analysis they were close to zero or slightly negative. This is probably a consequence of better representation of stratification and therefore the geographic distribution of salinity in this analysis than in the previous one (Kimmerer et al. 2009).

The relationships of habitat indices to X2 were remarkably similar among the species with predominantly freshwater or low-salinity affinities (Figure 8). Slopes had 10th and 90th percentiles of −0.1 to −0.22 for species not in the first row of Figure 8. This was a consequence of a general trend toward larger volume of water when volume was weighted using the resource selection functions. This contrasts with the bimodal distribution of volume within the LSZ. These resource–selection functions were either high in freshwater, and therefore responsive to the increase in volume of freshwater with increasing flow; or they were high across a broad range of

salinity, which likely averaged across the pattern observed for the LSZ (Figure 5).

Despite the similarity among the relationships of habitat index to X2, the abundance–X2 relationships (Kimmerer et al. 2009) differed greatly among the species (Figure 8). This finding, together with the lack of correspondence for some species between the habitat–X2 and abundance–X2 relationships (Figure 8), suggest that variation in the volume (or area, not shown) of physical habitat as defined by salinity is not a strong influence on abundance of many of these fish.

The lack of consistent parallels between the availability of salinity-based habitat and abundance could have had several causes. First, our use of salinity as the only variable that defines habitat is clearly inadequate. For example, turbidity is consistently important as a covariate in analyses of delta smelt distributions (Feyrer et al. 2007; Nobriga et al. 2008). Given the difficulty in determining the controls on the delta smelt population, it is not surprising that such a simple descriptor of habitat is inadequate for this species. Threadfin shad is more abundant in clearer water (Feyrer et al. 2009), which may limit its response to increases in freshwater flow and attendant changes in habitat. Other, unmeasured attributes of habitat such as food supply are likely to be important, but were outside the scope of our modeling effort.

Second, the mechanisms relating abundance to X2 may not involve the extent of suitable salinity. For example, longfin smelt are more abundant near the bottom than in the water column at high salinity, but not at low salinity. The mechanism behind this is unknown, but one possible result of this pattern is strong landward movement of the smelt in the deep channels, which may serve to retain the fish against net seaward flow.

As before, striped bass and American shad had relationships of habitat index to X2 that were similar to those for abundance. This is consistent with a mechanism by which abundance responds to quantity of habitat and thereby to flow (Jassby et al. 1995). However, the population of young striped bass does not expand spatially as X2 moves seaward, and several other mechanisms have been proposed for the response of this species to freshwater flow (Kimmerer et al. 2001).

Many aspects of habitat and its response to freshwater flow are missed or ignored by our analysis. As noted above, turbidity is related to abundance or feeding success of many visually-feeding estuarine fishes (e.g., Breitburg 1988; Aksnes and Utne 1997; Feyrer et al. 2007), but we lack a suitable turbidity model. Small-scale features such as fronts and bathymetric discontinuities are often sites of aggregation for fish and their prey (e.g., Cowen et al. 2000), and interactions between the salinity field and these features could be an important feature of habitat. Another important mechanism for the effects of flow on habitat for fish is stimulation of foodweb productivity, for example, through nutrient loading (Nixon 1988) or stratification (Skreslet 1997). Previous analyses have suggested that stimulation of phytoplankton production is an unlikely mechanism for the responses of nekton populations to flow (Kimmerer 2002b).

Despite the complexities, salinity is the most important variable for determining the locations of pelagic estuarine organisms and therefore their physical habitat (Mouny and Dauvin 2002; Jung and Houde 2003; Dege and Brown 2004; Kimmerer 2004). Our findings generally imply that extent of suitable salinity by itself is not a major determinant of the responses of abundance to flow for most of the estuarine species we examined. Dynamic attributes of habitat that vary with flow, such as retention by estuarine circulation or transport to rearing areas, may be more important than quantity of habitat for some fish species.

ACKNOWLEDGEMENTS

REFERENCES

Aksnes DL, Utne ACW. 1997. A revised model of visual range in fish. Sarsia 82(2):137–147.

Armor C, Herrgesell PL. 1985. Distribution and abundance of fishes in the San Francisco Bay estuary between 1980 and 1982. Hydrobiologia 129:211-227.

Arthur JA, Ball MD. 1979. Factors influencing the entrapment of suspended material in the San Francisco Bay–Delta estuary. In: Conomos TJ, editor. San Francisco Bay: the urbanized estuary. San Francisco (CA): Pacific Division, AAAS. p 143–174.

Attrill MJ, Rundle SD. 2002. Ecotone or ecocline: ecological boundaries in estuaries. Estuar Coast Shelf Sci 55(6):929–936.

Baross JA, Crump B, Simenstad CA. 1994. Elevated 'microbial loop' activities in the Columbia River estuarine turbidity maximum. In: Dyer KR, Orth RJ, editors. Changes in fluxes in estuaries: implications from science to management. Fredensborg, Denmark: Olsen & Olsen. p 459–464.

Bennett WA. 2005. Critical assessment of the delta smelt population in the San Francisco Estuary, California. San Fran Estuar Water Sci [Internet]. [cited 23 Oct 2013]; 3(2). Available from: http://www.escholarship.org/uc/item/0725n5vk

Bennett WA, Kimmerer WJ, Burau JR. 2002. Plasticity in vertical migration by native and exotic estuarine fishes in a dynamic low-salinity zone. Limnol Oceanogr 47(5):1496–1507.

Breitburg DL. 1988. Effects of turbidity on prey consumption by striped bass larvae. Trans Am Fish Soc 117(1):72–77.

Bulger AJ, Hayden BP, Monaco ME, Nelson DM, McCormick–Ray MG. 1993. Biologically-based estuarine salinity zones derived from a multivariate analysis. Estuaries 16(2):311–322.

Burau JR. 1998. Results from the hydrodynamic element of the 1994 entrapment zone study in Suisun Bay. In: Kimmerer WJ, editor. Report of the 1994 Entrapment Zone Study. Sacramento (CA): IEP for the San Francisco Estuary. p. 13–62.

Casulli V, Cattani E. 1994. Stability, accuracy and efficiency of a semi-implicit method for three-dimensional shallow water flow. Comput Math Appl 27(1):99–112.

Casulli V, Zanolli P. 2002. Semi-implicit numerical modeling of nonhydrostatic free-surface flows for environmental problems. Math Comput Model 36(9–10):1131–1149.

Casulli V, Zanolli P. 2005. High resolution methods for multidimensional advection–diffusion flows in free-surface hydrodynamics. Ocean Model 10(1):137–151.

Cloern J, Alpine A, Cole B, Wong R, Arthur J, Ball M. 1983. River discharge controls phytoplankton dynamics in the northern San Francisco Bay estuary. Est Coast Shelf Sci 16(4):415–429.

Cloern JE. 1984. Temporal dynamics and ecological significance of salinity stratification in an estuary (South San Francisco Bay, USA). Oceanol Acta 7(1):137–141.

Cowen RK, Lwiza KMM, Sponaugle S, Paris CB, Olson DB. 2000. Connectivity of marine populations: open or closed? Science 287(5454):857–859.

Dege M, Brown LR. 2004. Effect of outflow on spring and summertime distribution and abundance of larval and juvenile fishes in the upper San Francisco Estuary. In: Feyrer F, Brown LR, Brown RL, Orsi JJ, editors. Early life history of fishes in the San Francisco Estuary and watershed. Bethesda (MD): American Fisheries Society. p. 49–65.

Feyrer F, Nobriga ML, Sommer TR. 2007. Multi-decadal trends for three declining fish species: habitat patterns and mechanisms in the San Francisco Estuary, California, U.S.A. Can J Fish Aquat Sci 64(4):723–734.

Feyrer F, Sommer T, Slater SB. 2009. Old school vs. new school: status of threadfin shad (*Dorosoma petenense*) five decades after its introduction to the Sacramento–San Joaquin Delta. San Fran Estuary Water Sci [Internet]. [cited 23 Oct 2013]; 7(1). Available from: http://www.escholarship.org/uc/item/4dt6p4bv

Greenwood M. 2007. Nekton community change along estuarine salinity gradients: Can salinity zones be defined? Estuar Coast 30(3):537–542.

Grimaldo LF, Sommer T, Ark NV, Jones G, Holland E, Moyle PB, Herbold B, Smith P. 2009. Factors affecting fish entrainment into massive water diversions in a tidal freshwater estuary: can fish losses be managed? N Am J Fish Manage 29(5):1253–1270.

Gross ES, Koseff JR, Monismith SG. 1999. Three-dimensional salinity simulations of south San Francisco Bay. J Hydraul Eng 125(11):1199–1209.

Gross ES, MacWilliams ML, Kimmerer WJ. 2010. Three-dimensional modeling of tidal hydrodynamics in the San Francisco Estuary. San Fran Estuar Water Sci [Internet]. [cited 23 Oct 2013]; 7(2). Available from: *http://www.escholarship.org/uc/item/9rv243mg*

Hobbs JA, Bennett WA, Burton J, Gras M. 2007. Classification of larval and adult delta smelt to nursery areas by use of trace elemental fingerprinting. Trans Am Fish Soc 136(2):518–527.

Jassby AD, Kimmerer WJ, Monismith SG, Armor C, Cloern JE, Powell TM, Schubel JR, Vendlinski TJ. 1995. Isohaline position as a habitat indicator for estuarine populations. Ecol Appl 5(1):272–289.

Jung S, Houde ED. 2003. Spatial and temporal variabilities of pelagic fish community structure and distribution in Chesapeake Bay, USA. Estuar Coast Shelf Sci 58(2):335–351.

Kimmerer WJ. 2002. Effects of freshwater flow on abundance of estuarine organisms: physical effects or trophic linkages? Mar Ecol Progr Ser 243:39–55.

Kimmerer WJ. 2002. Physical, biological, and management responses to variable freshwater flow into the San Francisco Estuary. Estuaries 25(6B):1275–1290.

Kimmerer WJ. 2004. Open water processes of the San Francisco Estuary: from physical forcing to biological responses. San Fran Estuar Water Sci [Internet]. [cited 23 Oct 2013]; 2(1). Available from: *http://www. escholarship.org/uc/item/9bp499mv*

Kimmerer WJ, Bennett WA, Burau JR. 2002. Persistence of tidally-oriented vertical migration by zooplankton in a temperate estuary. Estuaries 25(3):359–371.

Kimmerer WJ, Burau JR, Bennett WA. 1998. Tidally-oriented vertical migration and position maintenance of zooplankton in a temperate estuary. Limnol Oceanogr 43(7):1697–1709.

Kimmerer WJ, Cowan JH, Miller LW, Rose KA. 2001. Analysis of an estuarine striped bass population: effects of environmental conditions during early life. Estuaries 24(4):556–574.

Kimmerer WJ, Gross ES, MacWilliams M. 2009. Is the response of estuarine nekton to freshwater flow in the San Francisco Estuary explained by variation in habitat volume? Estuar Coast 32(2):375–389.

Kimmerer WJ, Parker AE, Lidström U, Carpenter EJ. 2012. Short-term and interannual variability in primary production in the low-salinity zone of the San Francisco Estuary. Estuar Coast 35(4):913–929.

Lacroix G, Ruddick K, Ozer J, Lancelot C. 2004. Modelling the impact of the Scheldt and Rhine/Meuse plumes on the salinity distribution in Belgian waters (southern North Sea). J Sea Res 52(3):149–163.

Lucas LV, Koseff JR, Monismith SG, Cloern JE, Thompson JK. 1999. Processes governing phytoplankton blooms in estuaries. II: The role of horizontal transport. Mar Ecol Progr Ser 187:17–30.

Lucas LV, Thompson JK. 2012. Changing restoration rules: exotic bivalves interact with residence time and depth to control phytoplankton productivity. Ecosphere 3(12):Art. 17.

MacWilliams ML, Salcedo FG, Gross ES. 2008. San Francisco Bay–Delta UnTRIM model calibration report, POD 3-D particle tracking modeling study. Prepared for California Department of Water Resources, December 19, 2008. 344 p. Available from: *http://www.water.ca.gov/iep/docs/pod/UnTRIM_ Calibration_Report.pdf*

Manly BFJ, McDonald LL, Thomas DL, MacDonald TL, Erickson WP. 2002. Resource selection by animals: statistical design and analysis for field studies. New York (NY): Kluwer. 240 p.

Monismith SG, Kimmerer WJ, Burau JR, Stacey MT. 2002. Structure and flow-induced variability of the subtidal salinity field in northern San Francisco Bay. J Phys Oceanogr 32(11):3003–3019.

Morris AW, Mantoura RFC, Bale AJ, Howland RJM. 1978. Very low salinity regions of estuaries: important sites for chemical and biological reactions. Nature 274:678–680.

Mouny P, Dauvin J–C. 2002. Environmental control of mesozooplankton community structure in the Seine estuary (English Channel). Oceanol Acta 25(1):13–22.

Moyle PB, Herbold B, Stevens DE, Miller LW. 1992. Life history and status of the delta smelt in the Sacramento-San Joaquin Estuary, California. Trans Am Fish Soc 121:67–77.

Nichols FH. 1985. Increased benthic grazing: an alternative explanation for low phytoplankton biomass in northern San Francisco Bay during the 1976–1977 drought. Estuar Coast Shelf Sci 21(3):379–388.

Nixon SW. 1988. Physical energy inputs and the comparative ecology of lake and marine ecosystems. Limnol Oceanogr 33(4):1005–1025.

Nobriga M, Sommer T, Feyrer F, Fleming K. 2008. Long-term trends in summertime habitat suitability for delta smelt, *Hypomesus transpacificus*. San Fran Estuar Water Sci [Internet]. [cited 23 Oct 2013]; 6(1). Available from: *http://www.escholarship.org/uc/item/5xd3q8tx*

North EW, Houde ED. 2003. Linking ETM physics, zooplankton prey, and fish early-life histories to striped bass *Morone saxatilis* and white perch *M. americana* recruitment. Mar Ecol Progr Ser 260:219–236.

Postma VH, Kalle K. 1955. On the development of turbid zones in the lower course of rivers with special consideration of conditions in the lower Elbe. *Sond Deutsch Hydr Zeitschrift* 8:137–144.

Powell TM, Cloern JE, Huzzey LM. 1989. Spatial and temporal variability in south San Francisco Bay (USA). I. Horizontal distributions of salinity, suspended sediments, and phytoplankton biomass and productivity. Estuar Coast Shelf Sci 28(6):583–597.

Skreslet S. 1997. A conceptual model of the trophodynamical response to river discharge in a large marine ecosystem. J Mar Syst 12(1–4):187–198.

Sommer TR, Harrell WC, Matica Z, Feyrer F. 2008. Habitat associations and behavior of adult and juvenile splittail (Cyprinidae: *Pogonichthys macrolepidotus*) in a managed seasonal floodplain wetland. San Fran Estuar Water Sci [Internet]. [cited 23 Oct 2013]; 6(2). Available from: *http://www.escholarship.org/uc/item/85r15611*

Turner JL, Chadwick HK. 1972. Distribution and abundance of young-of-the-year striped bass, *Morone saxatilis*, in relation to river flow in the Sacramento–San Joaquin estuary. Trans Am Fish Soc 101:442–452.

Watson EB, Byrne R. 2009. Abundance and diversity of tidal marsh plants along the salinity gradient of the San Francisco Estuary: implications for global change ecology. Plant Ecol 205(1):113–128.

Wilber DH. 1992. Associations between freshwater inflows and oyster productivity in Apalachicola Bay, Florida. Estuar Coast Shelf Sci 35(2):179–190

Zimmerman JTF. 1986. The tidal whirlpool: a review of horizontal dispersion by tidal and residual currents. Neth J Sea Res 20(2–3):133–154.